

1 TITLE: Demogenetic simulations reveal fragmenting effects of climate change on insular lizard  
2 populations.

3

4 Stephen E. Rice<sup>1</sup> and Rulon W. Clark<sup>1</sup>

5 1. San Diego State University, Dept of Biology, 5500 Campanile Drive, San Diego, California,  
6 92182

7

8 CORRESPONDING AUTHOR:

9 Stephen E. Rice, San Diego State University, Department of Biology, 5500 Campanile Drive,  
10 San Diego, California, 92182-4614. Phone: (619) 594-2435 Fax: (619) 594-5676. Email:

11 srice001@ucr.edu

12

13 ACKNOWLEDGEMENTS

14 Support for this research came from United States Department of Defense (Award Number  
15 W9126G-12-2-0060) and the Southern California Research and Learning Center (Award  
16 Number S18309). We would like to thank the National Park Service for access to SBI, SCI  
17 Naval Base for access to SCI and our field assistants. In addition we would like to thank Drs. A.  
18 Bohonak (SDSU), H. Regan (UCR), K. Anderson (UCR), and J. Gatesy (UCR) for comments  
19 received during manuscript preparation.

20

## 21 **ABSTRACT**

22           The extinction risk of insular species with sessile life histories is expected to increase as  
23 they may be unable to track habitat in response to global climate change. Demogenetic  
24 simulations can couple population demography and niche modeling to produce spatially-explicit  
25 genetic and demographic information for all simulated individuals and provide insight into the  
26 effects of climate change at demographic and population genetic levels. We used CDMETAPOP  
27 to simulate a population of island night lizards (*Xantusia riversiana*) on Santa Barbara Island to  
28 evaluate its sensitivity to climate change to the year 2100 across 8 scenarios based on 2 climate  
29 models, 2 emissions pathways, and 2 connectivity models. We found that 1) *X. riversiana* is  
30 sensitive to climate change with SDMs predicting a loss of suitable habitat of 93%-98% by 2038,  
31 2) population genetic structure is expected to increase drastically to 0.209-0.673 from  
32 approximately 0.0346, and 3) estimated minimum abundance is expected to decline sharply  
33 over the 2007 to 2038 period and reached values of 0-1% of the 2007 population size in all  
34 scenarios by 2100. Climate change is expected to decrease census population size and result in  
35 extant habitat patches that are isolated from one another with very high levels of genetic  
36 divergence over short periods of time. These patterns may drive the Santa Barbara Island  
37 population to extinction under certain scenarios. Management plans should address methods to  
38 improve connectivity on the island and attempt to create refugial patches. Contingency plans,  
39 such as translocation, may be required to prevent population extirpation. This study highlights  
40 the utility of demogenetic simulations in evaluating population demographic and genetic patterns  
41 under climate change with suggestions on workflows for running simulations in a high-  
42 throughput manner.

43

## 44 **INTRODUCTION**

45           Global climate change may lead to rapid changes in environmental conditions, thus  
46 presenting unique challenges to species persistence. Climate change is expected to strongly  
47 affect species with restricted ranges, specialized niches, limited dispersal ability, and small  
48 effective population sizes (Oliver and Morecroft 2014), conditions intrinsic to many insular  
49 species. Populations may respond to climate change by tracking habitat shifts, coping through  
50 phenotypic plasticity or adaptation, or failing these, may go extinct (Penuelas et al. 2013). The  
51 persistence of populations is thereby directly related to organisms' abilities to track suitable

52 habitat or cope with changing conditions. For insular species, climate change may shift suitable  
53 niche space outside of the dispersal threshold and may result in sharp population declines,  
54 increased selective pressures, or extinction.

55 Species sensitivity to climate change has been assessed through multiple modeling  
56 approaches, which range from species distribution models (SDMs) to stochastic simulations  
57 linking population demography to SDM predictions (e.g. Fordham et al. 2012; Swab et al. 2015).  
58 While effective tools for assessing population viability, these approaches do not incorporate  
59 genetic population structure, diversity estimates, and do not include scenarios for adaptation.  
60 Recent advances in individual-based simulations have led to landscape demogenetic models  
61 (Landguth et al. 2017a) which allow for a greater range of questions and scenarios to be  
62 investigated that incorporate demographic and genetic data.

63 Studies which use demogenetic models to investigate the effects of environmental  
64 change have been primarily focused on aquatic systems (e.g. Landguth et al. 2014; Piou et al.  
65 2015). The use of detailed demogenetic models for climate change assessments in terrestrial  
66 systems remains largely unexplored. The flexibility of this modeling approach allows the  
67 coupling of population demography with SDM predictions to investigate the effects of climate  
68 change on population viability while also providing data to describe population genetic patterns.  
69 In addition to their flexibility, demogenetic models can simulate genetic data equivalent to  
70 empirical approaches which provide benchmarks for model parameterization (e.g. Row et al.  
71 2014).

72 Islands provide exemplary systems for evaluating the use of demogenetic simulations in  
73 assessments of terrestrial systems due to their natural isolation and limited spatial extent. These  
74 attributes allow fine-scale simulations of closed populations to determine the sensitivity of  
75 insular species to climate change while simultaneously evaluating the practical constraints of  
76 demogenetic simulations. Recent research on the island night lizard, *Xantusia riversiana*, has  
77 characterized genetic patterns across two-thirds of the species range, found correlations of  
78 landscape features with genetic structure, and characterized dispersal patterns (Rice and Clark  
79 2016, 2017) which provide empirical benchmarks for the parameterization of demogenetic  
80 models. Previous ecological research identified precipitation as an important variable in  
81 reproduction and calculated habitat-specific carrying capacities (Fellers and Drost 1991),  
82 suggesting a coupling of demography and climatic suitability. The island night lizard is one of

83 the few reptiles endemic to the California Channel Islands; however, climate change sensitivity  
84 has yet to be assessed due to an expectation of limited effect on these locally abundant  
85 populations (United States Fish and Wildlife Service (USFWS) 2014). The combination of  
86 closed and well-characterized populations with the need for climate change sensitivity analyses  
87 presents a compelling opportunity to apply demogenetic simulations to this insular system.

88 We constructed demogenetic models in the program CDMETAPOP (Landguth et al.  
89 2017a) for island night lizards on Santa Barbara Island (SBI) to determine the effects of climate  
90 change on expected minimum abundances (EMA), quasi-extinction risks, and population genetic  
91 structure. We used stochastic simulations which included demographic and environmental  
92 stochasticity to assess population sensitivity to climate change. We modeled the effects of  
93 climate change through annual changes in patch carrying capacity and evaluated the sensitivity  
94 of extinction risk and population genetic patterns to variability in the effective distances between  
95 patches due to climate change. Finally, we evaluated the practicality of using demogenetic  
96 models to conduct these analyses and identified approaches to improve these models in terrestrial  
97 systems.

98

## 99 **METHODS**

### 100 *Study Species*

101 *Xantusia riversiana* is the only reptile endemic to three California Channel Islands: SBI,  
102 San Clemente Island (SCI), and San Nichols Island. Each island is a distinct evolutionary and  
103 management unit (USFWS 2014). Two subspecies were recognized by Smith (1946), with SBI  
104 and SCI populations grouped as *X. r. reticulata* and San Nichols Island recognized as *X. r.*  
105 *riversiana* based on morphology. In addition to morphology, the San Nichols Island population  
106 differs in habitat utilization, body size, and reproductive rates (Fellers et al. 1998). Island night  
107 lizards are habitat generalist on SBI and SCI with the greatest densities occurring in California  
108 boxthorn (*Lycium californicum*), prickly pear cactus (*Opuntia littoralis*), and rocky habitats  
109 (Fellers and Drost 1991; Mautz 1993). Population densities in prime habitat are estimated to be  
110 in excess of 3,200 individuals/ha with total population sizes on SCI estimated at 21.3 million and  
111 17,600 on SBI (USFWS 2014). Individuals on SCI may live in excess of 23 years (Mautz 2015,  
112 pers. comm) with sexual maturity reached between 2 and 3 years (Fellers and Drost 1991;  
113 Goldberg and Bezy 1974). Reproduction is is influenced by precipitation patterns and

114 hypothesized to occur biennially for mature females (Fellers and Drost 1991). Geographic  
115 distance and landscape features were correlated with genetic distance on SBI and SCI (Rice and  
116 Clark 2016). Landscape features included negative correlations with prime habitat and positive  
117 correlations with canyons, secondary roadways, and coastal cholla cactus (*Cylindropuntia*  
118 *prolifera*) on SCI and wooly seablite (*Suaeda taxifolia*), crystalline iceplant  
119 (*Mesembryanthemum crystallinum*), and barren ground on SBI. Estimates of dispersal distance  
120 range from an average displacement of 3m (Mautz 1993) to genetically inferred dispersal  
121 ranging from 14m on SBI to 41m on SCI (Rice and Clark 2017). Island night lizards were  
122 delisted from threatened status under the Endangered Species Act in 2014, contingent on post-  
123 delistment monitoring. Climate change sensitivity has not been assessed for the species but is  
124 anticipated to be of minimal impact (USFWS 2014).

#### 125 *Habitat Suitability Models*

126 We constructed SDMs in MAXENT (Phillips et al. 2006) to identify contemporary  
127 correlates of climatic niche with occurrences limited to SCI and SBI, due to shared ecological  
128 and life history patterns. We used occurrence data from capture data (Rice and Clark 2016) and  
129 GBIF ([doi:10.15468/dl.rie3zo](https://doi.org/10.15468/dl.rie3zo)). We removed records without GPS coordinates, those that  
130 mapped outside of SBI and SCI, and those prior to 1959 to limit occurrence records to those  
131 which potentially overlap historic climate data. The occurrence data of Rice and Clark (2016)  
132 were spatially biased by distance to trails (SBI) and distance to roadways (SCI); therefore, we  
133 constructed bias maps using the distance of a cell to primary access route to assign probabilities  
134 of sampling a given cell. The probability of a given cell being sampled was the proportion of the  
135 cell's distance bin among all raster cells for each respective island.

136 Climatic predictors were the first 19 bioclim variables generated from 800 m<sup>2</sup> historical  
137 (1981-2010) PRISM precipitation and temperature data (PRISM 2012) using the R package  
138 DISMO (Hijmans et al. 2017). Terrain predictors of slope, aspect, terrain roughness, terrain  
139 ruggedness, and topographic position were constructed from a 10 m resolution National  
140 Elevation Dataset (United States Geological Survey 2017) and resampled to 100 m using the R  
141 package RASTER (Hijmans et al. 2016). Highly correlated predictors were removed through  
142 stepwise variance inflation factor (VIF) analysis in the R package USDm (Naimi 2015) with a  
143 threshold of 10. Cleaned occurrence data was used with retained predictors to construct SDMs

144 using the autofeatures setting, duplicate occurrence records removed, and bootstrapped 1000  
145 times (Franklin 2010).

146 Two global climate models were chosen for the projection of SDMs to future time  
147 periods. The two models, CanESM and Miroc, are considered predictive for the Basic  
148 Characterization Model, which informs many California climate assessments (Flint et al. 2013).  
149 The CanESM and Miroc climate models, at representative concentration pathways (RCPs) of 4.5  
150 and 8.5, were downscaled to 100 m resolution by Dr. Alan Flint (USGS) for monthly  
151 temperature and precipitation variables. We constructed bioclim variables for projections to the  
152 years 2038, 2069, and 2100 by averaging monthly variables over the 30 years prior to each time  
153 point and using these averages to produce bioclim predictors. Terrain variables remained  
154 unchanged in all scenarios. The bootstrapped SDMs were projected to each time point and  
155 averaged to identify habitat suitability under climate change scenarios. We defined the  
156 contemporary habitat suitability map as the year 2007 for all downstream analyses and  
157 interpolations, which allowed consistent 30 year time spans for all endpoint projections.

#### 158 *Demogenetic Simulations*

159 We modeled the effects of climate change on population viability and genetic structure  
160 using the demogenetic modeling approach of Landguth et al. (2017) with the program  
161 CDMETAPOP. Demogenetic models included climate change as a process which modified the  
162 habitat suitability of each raster cell. The effect of climate change on population viability was  
163 investigated by linking patch carrying capacities to habitat suitability values. Additionally, we  
164 parameterized two resistance surface models to evaluate the effect of climate change on inter-  
165 patch connectivity. Two resistance surface models were evaluated, a static model based on  
166 geographic distance and a dynamic model based on habitat suitability. We linearly interpolated  
167 between each endpoint to produce annual SDMs ranging from 2007 through the year 2100 using  
168 RASTER. We modeled every 1 ha raster cell as a distinct patch with a constant relationship  
169 between carrying capacity and habitat suitability. The constant relationship between individuals  
170 and habitat suitability was determined by taking the census population size and dividing by the  
171 sum of contemporary habitat suitability. Populations on SBI were modeled with patch carrying  
172 capacities determined by habitat suitability multiplied by the constant of 117.76 individuals.

173 Demographic parameters were drawn from the ecological literature of *X. riversiana*  
174 (Fellers and Drost 1991; Mautz 1993) and *X. vigilis* (Zweifel and Lowe 1966). *Xantusia*

175 *riversiana* exist in age structured populations; however, there is insufficient data to estimate the  
176 survival parameters needed to model demography. We used a 4-stage model (Table S1) of  
177 demography informed by survival estimates of a sister species, *X. vigilis*, which occur on the  
178 mainland. Both species display similar patterns of high juvenile survival (Mautz 1993) and  
179 reproductive potential (Goldberg and Bezy 1974). Fecundity values for *X. riversiana* from  
180 Fellers and Drost (1991) were used as parameters (Table S1) for reproductively active (4<sup>th</sup> stage)  
181 females which were modeled as seasonally monogamous with strict biennial reproduction.

182 All models included environmental and demographic stochasticity. Environmental  
183 stochasticity was incorporated through standard deviations in patch carrying capacity. The  
184 standard deviation for each patch at each time step was determined by applying the proportion of  
185 the standard deviation to mean population density on San Clemente Island, 0.1415 (Mautz 1993).  
186 Demographic stochasticity was modeled through all time steps as variability in survival rates and  
187 fecundity. Survival rate variability was modeled through the standard deviation in survival rates  
188 for each age group as estimated from Table 4 in Zweifel and Lowe (1966). Variability in  
189 fecundity was modeled by assigning the offspring number for each female from a normal  
190 distribution around the mean with standard deviation (Fellers and Drost 1991).

191 We used the same cost distance matrices and dispersal formula parameters and  
192 thresholds for mating and movement for both sexes. The cost distance matrices for each time  
193 step consisted of the effective resistance distances between all patches as calculated by the  
194 program CIRCUITSCAPE (McRae and Beier 2007). The static model based on geographic distance  
195 was constructed with a raster map with all terrestrial cells assigned a neutral value of 1, which  
196 constrained dispersal paths to land and has been shown to approximate log-transformed  
197 geographic distance (Lee-Yaw et al. 2009). Dynamic resistance maps, which assessed changes in  
198 connectivity, were produced for each time step with resistance set as the inverse of the habitat  
199 suitability for each raster cell. We modeled movements with a negative exponential function  
200 (scale =1.0, shape =0.75) and a maximum effective resistance distance threshold of 0.555 for  
201 geographic distance models and 1.25 for connectivity models. These values were chosen as they  
202 resulted in equilibrated global  $F_{st}$  estimates similar to the observed empirical value of 0.0346  
203 (Rice and Clark 2016) when modeled on the contemporary suitability map for 450 years. In  
204 addition to the 4 climate change scenarios, we modeled a “no change” scenario in which  
205 contemporary habitat suitability remained the same throughout the simulation.



206 We simulated 17,600 individuals with 20 microsatellite loci each with 15 alleles and no  
207 mutation. Simulations began with a panmictic population and equilibrated on contemporary  
208 conditions for 450 years to produce a 2007 estimate of global  $F_{st}$  approximate to the empirical  
209 data. Changes in carrying capacity and effective resistance distance began at the 2008 time step.  
210 Populations were fully sampled at the years 2038, 2069, and 2100 and global  $F_{st}$  calculated in  
211 the R package DIVERSITY (Keenan et al. 2013). Full census data was extracted for each timestep  
212 between 2007 and 2100 and was used to calculate proportional EMA, compared to 2007, and  
213 generate quasi-extinction graphs following McCarthy and Thompson (2001). All scenarios were  
214 replicated 100 times and ran on a high performance computational (HPC) cluster.

215

## 216 **RESULTS**

### 217 *Habitat Suitability*

218 Seven Bioclim variables and 3 terrain variables were retained by stepwise VIF (Table 1)  
219 resulting in a maximum correlation between Bio5 and Bio9 of 0.7706. Maximum temperature in  
220 the warmest month, Bio5, had the most useful information by itself and topographic position  
221 index (TPI) had the most information not present in other variables. The minimum observed  
222 habitat suitability value for any occupancy record was 0.1095, which was used as the threshold  
223 definition to visualize habitat patches (Supplemental Figures S1-S13) and differentiate suitable  
224 from unsuitable habitat patches. All climate scenarios displayed striking decreases in suitable  
225 habitat availability and distribution. These models predict 93.13%-99.81% reductions in suitable  
226 habitat on SBI and SCI from 2007 under all scenarios for the year 2038 (Figure 1), which  
227 correspond to a change from 7482 ha under current conditions to 514 - 14 ha under climate  
228 change. Suitable habitat expanded on a nearby island to the east of SBI and SCI, Santa Catalina,  
229 which is outside of the current and historic species distribution. The Miroc 8.5 model retained  
230 the most suitable habitat on SCI and SBI combined. Habitat suitability for all scenarios declined  
231 through the year 2069 and declined to 0 suitable hectares under both CanESM scenarios and the  
232 Miroc 4.5 scenario by the year 2100. The Miroc 8.5 scenario was the only scenario investigated  
233 which did not result in the complete elimination of suitable habitat.

### 234 *Demogenetic Simulations*

235 All models equilibrated at global  $F_{st}$  values (Figure 2) similar to the empirical data of  
236 Rice and Clark (2016). The distance only models revealed sharp increases in global  $F_{st}$  across all



237 climate scenarios. Mean global  $F_{st}$  was approximately 0.043 at the 2007 time step in equilibrated  
238 models and increased to a range of 0.209-0.330 by 2100 depending on the model (Figure 2, top).  
239 The CanESM 8.5 model could not be assessed at the year 2100 due to population extinction  
240 throughout the simulations. EMA revealed sharp population declines (Figures 3-5, top) at all  
241 time points with the Miroc 8.5 projection being the most optimistic with 1.76% of the 2007  
242 population remaining by 2100 (Table 2). The CanESM 8.5 model resulted in complete extinction  
243 and the remaining models ended the century with  $\leq 0.15\%$  of the 2007 population remaining.  
244 Quasi-extinction graphs (Figures 3-5, top) also show increased extinction risks at 2038 with  
245 sharp increases in extinction risk through the end of the century. Connectivity models revealed  
246 the same trends and model rankings in global  $F_{st}$  as distance models; however values were  
247 almost twice as great (Figure 2, bottom). Mean global  $F_{st}$  values for connectivity models ranged  
248 from 0.5318-0.6733 by 2100 with CanESM 8.5 absent due to extinction. EMA and quasi-  
249 extinction analyses for connectivity models returned the same trends as distance models at  
250 similar values with the CanESM 8.5 model again resulting in extinction (Table 2, Figures 3-5,  
251 bottom).

252

## 253 **DISCUSSION**

254 SDMs can offer insight into the predicted shifts in habitat suitability for a species under  
255 climate change projections assuming that contemporary correlations hold (Franklin 2010). When  
256 combined with demogenetic simulations, these models allow for a spatially-explicit investigation  
257 into the effects of climate change on population demographic and genetic patterns. The current  
258 monitoring framework for the island night lizard suggests that climate change is not a concern  
259 for this species (USFWS 2014); however, our results indicate this species may be heavily  
260 impacted by climate change with reductions in suitable habitat and steep declines in population  
261 abundance. Under all climate change scenarios, SDMs predict a 93.13%-99.81% loss of suitable  
262 habitat on SBI and SCI. We investigated the sensitivity of *X. riverisiana* to climate change on  
263 SBI following a coupled niche-population model framework to determine the effects of climate  
264 change on population abundance and population genetic structure. We found global  $F_{st}$  values  
265 increased from the 2007 time point by factors of 4.76-7.55 for models with only geographic  
266 distance and 14.23-18.31 for models where climate change modified the intervening matrix.  
267 EMA revealed stark decreases in abundances across all climate models beginning in the year

268 2038 and extending until the end of the century. EMA at the year 2100 reached extinction for the  
269 CanESM 8.5 scenario and a maximum of 1.76% of the 2007 population under the Miroc 8.5  
270 model with a distance only dispersal scenario. EMA values for other climate models were <1%  
271 by 2100 (Table 2).

### 272 *Habitat Suitability*

273 The SDMs for *X. riversiana* represent the first efforts to characterize changes in habitat  
274 suitability for reptiles on the California Channel Islands. These models were correlative models  
275 built with abiotic factors and thus do not include vegetation or soil characteristics which may  
276 contribute towards the true suitability of habitat to support island night lizard populations.  
277 MAXENT is considered one of the most accurate SDM methods but may lead to more pessimistic  
278 projections than other methods (Conlisk et al. 2013). Even with these limitations, the  
279 contemporary SDM offered key insights into climatic factors which correlate with *X. riversiana*  
280 distributions on SBI and SCI. Precipitation is positively correlated with reproduction and  
281 recruitment on island and mainland *Xantusia* species (Fellers and Drost 1991; Zweifel and Lowe  
282 1966). Precipitation was incorporated in this SDM through the bioclim suite of variables which  
283 include interactions between temperature and precipitation. The largest contributing variable to  
284 these models was Bio9, the mean temperature in the driest quarter, which corresponded to  
285 summer, June through August, on the California Channel Islands and overlaps with the  
286 gestational period of *X. riversiana* (Goldberg and Bezy 1974). The climatic niche and tolerances  
287 of *X. riversiana* are poorly understood, including the effects of temperature and water  
288 availability on successful gestation, and this variable may represent physiological constraints  
289 associated with gestation and realized climatic niche. Further experimental research is needed to  
290 examine the hypothesis that reproductive physiology and environmental constraints on gestation  
291 limit this species climatic niche.

292 SDMs projected under the Miroc and CanESM climate models revealed similar trends  
293 across both RCPs. The greatest decline in suitable habitat occurred between the contemporary  
294 model and 2038. The steepness of this decline, a loss of approximately 93% - 99% of  
295 contemporary habitat, is jarring given the longevity of the species and recent delistment. While  
296 these values may be pessimistic, they offer a clear indication that climate change is projected to  
297 have much larger effects on insular species within the California Floristic Province than included  
298 in current management plans. Based on the sensitivity of this highly abundant insular reptile, we

299 recommend that species management and conservation efforts on the California Channel Islands  
300 incorporate habitat suitability forecasts, as habitat tracking may be an inviable option for strictly  
301 terrestrial species which may require translocation and assisted colonization to prevent extinction  
302 under climate change.

### 303 *Demogenetic Simulations*

304 Individual-based spatially explicit demogenetic models are a recent tool which may give  
305 insight into processes generating population genetic patterns and population demographic  
306 trajectories. Previous research with CDMETAPOP is limited due to the recent publication of the  
307 method (Landguth et al. 2017a) but has included evaluation of blister rust resistance scenarios in  
308 whitebark pine (Landguth et al. 2017b) and invasive species management (Landguth et al.  
309 2017a). However, CDMETAPOP is built modularly to draw on previous individual-based  
310 spatially-explicit models, such as CDPOP (Landguth and Cushman 2010), which have been  
311 utilized to explore topics ranging from climate change sensitivity in Lynx (Row et al. 2014) to  
312 experimental design (Rico 2017). Demogenetic simulations conducted with CDMETAPOP may  
313 be parameterized to yield coupled niche-population models with genetic data which can enhance  
314 research into the effects of connectivity, population structure, or adaptation under changing  
315 climate. Demogenetic simulations may improve coupled niche population modeling efforts by  
316 providing greater insight into the effects of climate change but the tradeoffs of this approach  
317 include increased computational time, computational load, and can be labor intensive to  
318 parameterize and analyze.

319 We approached demogenetic simulations from the framework of coupled niche  
320 population models by linking habitat suitability values with patch carrying capacity and varying  
321 that carrying capacity at each time step. Additionally, we explored the effect of modeling  
322 effective resistance between patches as a function of annual habitat suitability and compared this  
323 approach to a more traditional approach assuming geographic distance alone. We found  
324 demogenetic simulation to be a computationally expensive tool that provided insight into  
325 population viability and genetic structure under multiple climate change and effective distance  
326 scenarios. The scale of this study was only possible through the use of a HPC cluster to increase  
327 model throughput during parameterization and simulation, and would have been intractable on a  
328 standard workstation due to processing time and the storage space required for simulations and  
329 analyses (>1 TB for this study). The ability to run CDMETAPOP across multiple cores of a

330 computer cluster and deploy basic R scripts to adjust model parameters and analyze simulated  
331 data allowed model parameterization and simulations to occur in a high-throughput manner  
332 which was only limited by computer usage quotas. Demogenetic models constructed for SBI  
333 were 17,600 individuals spread across 247 1 ha patches for a time period 542 years. A single  
334 iteration could complete on a single processor with 2GB of memory in 8-12 hours. This  
335 partitioning of computational load across multiple cores allowed an increase in the number of  
336 model runs, but still only a fraction of the number used in traditional coupled niche population  
337 models (e.g. Conlisk et al. 2013, Swab et al. 2015). However, the number was similar to other  
338 demogenetic approaches (e.g. Landguth et al. 2014; Piou et al. 2015). The parameterization and  
339 execution of simulations on a computer cluster is recommended to ensure robust examination of  
340 parameter space, and will be essential if modeling changes in genetic patterns from an assumed  
341 equilibrium in species of high density and continuous distribution.

342 Failure to validate equilibrium conditions for global  $F_{st}$ , and presumably other genetic  
343 metrics, when parameterizing models may lead to spurious and incorrect inferences. The current  
344 configuration of CDMETAPOP prevents parallelization and we found that the computational load  
345 becomes intractable for millions of individuals. Our attempts to parameterize models of SCI  
346 revealed that even at 10% of the census population size (2.15 million) two computer cores given  
347 15 GB of RAM on a computer cluster were unable to generate the initial population in a 24 hour  
348 period. Furthermore, we found that efforts to parameterize models based on reducing the  
349 modeled population to the effective population size at each collection site failed to reach  
350 equilibrium of global  $F_{st}$  values even when dispersal was set to the maximum threshold. While  
351 we could achieve values equivalent to empirical values, these values were not stable and  
352 continued to increase even as effective distance and carrying capacity remained stationary.  
353 Failure to validate the assumed pattern or compare would have led to a serious inference error on  
354 the magnitude of change expected under climate change scenarios.. In addition to validating  
355 equilibrium conditions when examining questions of genetic structure, researchers may be forced  
356 to examine various simulated population sizes or spatial extents based on computational  
357 constraints.

### 358 *Implications for Conservation*

359 The current distribution of *X. riversiana* will likely constrain its ability to cope with  
360 climate change through habitat tracking due to insular populations and dispersal distances under

361 50 m on both SBI and SCI. The projected size of habitat available to island night lizards based  
362 on SDM predictions is concerning due to the sharp declines in suitable habitat by 2038 in all  
363 scenarios and continued decline through the end of the century. Conservation efforts on both  
364 islands should focus on the creation of refugia/management areas in regions predicted to be the  
365 most suitable across climate predictions in an effort to ameliorate the anticipated loss of suitable  
366 habitat over the next 2 decades. Demogenetic simulations on SBI revealed populations are  
367 sensitive to climate change across all climate change scenarios when climate influences carrying  
368 capacities. We found that global  $F_{st}$  as a metric of intra-island isolation of patches were more  
369 sensitive to the resistance of the intervening matrix whereas demographic patterns represented by  
370 EMA were not. Rice and Clark (2016) found landscape correlates with genetic distance on SCI  
371 and SBI in addition to geographic distance. Simulation levels of global  $F_{st}$  suggest that even in  
372 scenarios of stable geographic distance, isolation of populations poses a major concern as global  
373  $F_{st}$  values corresponded to significant population structure (Figure 2). These findings suggest  
374 that populations may be threatened by climate change through habitat loss, habitat degradation,  
375 and isolation of suitable patches. Increased isolation of patches even within a small island may  
376 further increase the extinction risk of the species through inbreeding depression or Allee effects.  
377 Based on SDM and simulation predictions, management intervention may be required to prevent  
378 extinction of *X. riversiana* on SBI as early as 2038. While we were unable to model SCI in  
379 demogenetic simulations, we expect similar patterns to hold given the shared life history traits  
380 and prime habitat requirements. The census population size is greater on SCI than SBI, thus the  
381 risk of quasi-extinction is likely reduced but sharp declines in population abundance are  
382 anticipated based on the loss of suitable habitat indicated by SDMs (Figures S1-S13).

383 Recommended management interventions include increasing prime habitat of California  
384 boxthorn and prickly pear cactus in areas of greater projected habitat suitability and between  
385 populations identified by Rice and Clark (2016) to serve as potential refugia and improved  
386 connectivity among populations. As a generalist species, the simulated responses of *X. riversiana*  
387 on SBI may be indicative of increased threats to plant communities or endemic deer mouse  
388 populations from climate change and a lack of viable habitat tracking. This study is specific to  
389 island night lizards, but highlights a need for further study among insular species for which  
390 climate change sensitivity analyses are lacking.

391 *Conclusions*

392           Based on the results of demogenetic modeling, island night lizards are at high risk from  
393 climate change over the next several decades. The demographic effects of climate change over a  
394 range of emission and model scenarios are predicted to cause sharp population declines through  
395 decreased carrying capacities and sharp increases in population structure even when only  
396 geographic distance between patches is considered. We recommend that the National Park  
397 Service, the managing entity of SBI, and other agencies continue to monitor habitat and  
398 population sizes and key climatic variables to determine if populations begin to decline as  
399 predicted by our models. Additional factors may add to persistence of *X. riversiana* populations  
400 under climate change, such as responses of vegetation or soil characteristics necessary to  
401 maintain thermoregulation or unidentified plasticity within the species that could buffer against  
402 declines. These modeling results are also subject to the limitations of the method, chiefly that we  
403 assume the niche of island night lizards is well described by environmental variables, that  
404 contemporary relationships hold in future scenarios, and that population demography is  
405 monotonically coupled to habitat suitability. While these assumptions are likely violated, further  
406 research is needed into the sensitivity of model predictions to changes in population size, SDM  
407 construction, and parameters associated with vital rates. Additional research with demogenetic  
408 simulations within this system should address hypotheses related to adaptive responses to heat  
409 and drought tolerance, which can be implemented within the demogenetic models.

410           Demogenetic models are a valuable tool for climate change sensitivity analyses, but  
411 their usage is constrained to populations consisting of tens of thousands. Parameterization of  
412 models to yield genetic patterns which approximate empirical conditions under equilibrium  
413 settings can highlight model sensitivities to the spacing and densities of populations while  
414 providing benchmarks for model parameterization. We found stochastic simulations were  
415 informative to evaluate the sensitivity of an island population to environmental and demographic  
416 stochasticity as well as the permeability of the intervening matrix and provide insight into the  
417 genetic and demographic trajectories this species may face during the remainder of the century.  
418 While 100 stochastic simulations is below the traditional population viability analyses, it is  
419 equivalent to previous work with demogenetic simulations. Leveraging HPC clusters should  
420 alleviate some of the computational constraints for more robust simulation sizes. We recommend  
421 researchers interested in demogenetic simulations pursue HPC solutions to allow for increased  
422 simulations and robust model inferences. Secondary constraints are the computational load of



423 analyzing simulated data and will vary with the research being conducted. Estimation of  
424 extinction risk and temporal trends in population size are easily extracted from summary tables  
425 within simulations; however metrics of population structure, such as global  $F_{st}$ , require more  
426 effort and considerably more time to extract. As demogenetic simulations grow in usage,  
427 dedicated workflows will need to emerge to reduce computational loads and provide an  
428 implementation to conduct thorough sensitivity analyses on the effect of model parameters.

429

#### 430 **LITERATURE CITED**

431 Conlisk, E., Syphard, A. D., Franklin, J., Flint, L., Flint, A., & Regan, H. (2013). Uncertainty in  
432 assessing the impacts of global change with coupled dynamic species distribution and  
433 population models. *Global Change Biology*, 19(3), 858–869.

434 <https://doi.org/10.1111/gcb.12090>

435 Fellers, G. M., & Drost, C. A. (1991). Ecology of the Island Night Lizard, *Xantusia riversiana*,  
436 on Santa Barbara Island, California. *Herpetological Monographs*, 5, 28.

437 <https://doi.org/10.2307/1466975>

438 Fellers, G. M., Drost, C. A., Mautz, W. J., & Murphey, T. G. (1998). Ecology of the Island Night  
439 Lizard, *Xantusia riversiana*, on San Nicolas Island, California (Report) (p. 80). Retrieved  
440 from <http://pubs.er.usgs.gov/publication/96678>

441 Flint, L.E., Flint, A. L., Thorne, J. H., & Boynton, R. (2013): Fine-scale hydrologic modeling for  
442 regional landscape applications: the California Basin Characterization Model  
443 development and performance. *Ecological Processes*, 2, 25. doi:10.1186/2192-1709-2-25

444 Fordham, D. A., Watts, M. J., Delean, S., Brook, W. B., Heard, L. M. B., & Bull, C. M. (2012).  
445 Managed relocation as an adaptation strategy for mitigating climate change threats to the  
446 persistence of an endangered lizard. *Global Change Biology*, 18, 2743-2755.

447 <http://10.1111/j.1365-2486.2012.02742.x>

448 Franklin, J. (2010). Mapping species distributions: spatial inference and prediction. Cambridge;  
449 New York: Cambridge University Press. Retrieved from

450 <http://dx.doi.org/10.1017/CBO9780511810602>

451 Goldberg, S. R., & Bezy, R. L. (1974). Reproduction in the island night lizard, *Xantusia*  
452 *riversiana*. *Herpetologica*, 350–360.

- 453 Hijmans, R. J., Phillips, S., Leathwick, J., & Elith, J. (2017). R package: "dismo": [https://cran.r-](https://cran.r-project.org/package=dismo)  
454 [project.org/package=dismo](https://cran.r-project.org/package=dismo)
- 455 Hijmans, R. J., van Etten, J., Cheng, J. Mattiuzzi, M., Sumner, M., Greenberg, A., Lamigueiro,  
456 O. P., Bevan, A., Racine, E. B., & Shortridge, A. (2016). R package: "raster":  
457 <https://cran.r-project.org/package=raster>
- 458 Keenan, K., McGinnity, P., Cross, T. F., Crozier, W. W., and Prodohl, P. A. (2013). An R  
459 package for the estimation of population genetics parameters and their associated errors.  
460 *Methods in Ecology and Evolution*, 4(8), 782-788. <https://doi.org/10.1111/2041-210X.12067>
- 461 Landguth, E. L., & Cushman, S. A. (2010). CDPOP: a spatially explicit cost distance population  
462 genetics program. *Molecular Ecology Resources*, 10(1), 156-161. [https://doi.org/10.1111/j.1755-](https://doi.org/10.1111/j.1755-0998.2009.02719.x)  
463 [0998.2009.02719.x](https://doi.org/10.1111/j.1755-0998.2009.02719.x)
- 464 Landguth, E. L., Bearlin, A., Day, C. C., & Dunham, J. (2017a). CDMetaPOP: an individual-  
465 based, eco-evolutionary model for spatially explicit simulation of landscape  
466 demogenetics. *Methods in Ecology and Evolution*, 8(1), 4–11.  
467 <https://doi.org/10.1111/2041-210X.12608>
- 468 Landguth, E. L., Holden, Z. A., Mahalovich, M. F., & Cushman, S. A. (2017b). Using landscape  
469 genetics simulations for planting blister rust resistant whitebark pine in the US Northern  
470 Rocky Mountains. *Frontiers in Genetics*, 8, 9.  
471 <https://dx.doi.org/10.3389/fgene.2017.00009>
- 472 Landguth, E. L., Muhlfeld, C. C., Waples, R. S., Jones, L., Lowe, W. H., Whited, D., Lucotch, J.,  
473 Neville, H., & Luikart, G. (2014). Combining demographic and genetic factors to assess  
474 population vulnerability in stream species. *Ecological Applications*, 24(6), 1505–1524.
- 475 Lee-Yaw, J. A., Davidson, A., Mcrae, B. H., & Green, D. M. (2009). Do landscape processes  
476 predict phylogeographic patterns in the wood frog? *Molecular Ecology*, 18(9), 1863–  
477 1874. <https://doi.org/10.1111/j.1365-294X.2009.04152.x>
- 478 Mautz, W. J. (1993). Ecology and energetics of the island night lizard, *Xantusia riversiana*, on  
479 San Clemente Island, California. In F. Hochberg (Ed.), *Third California Islands*  
480 *symposium: Recent advances in research on the California Islands* (pp. 417–428). Santa  
481 Barbara, CA: Santa Barbara Museum of Natural History.
- 482 McCarthy, M. A., & Thompson, C. (2001). Expected minimum population size as a measure of  
483 threat. *Animal Conservation*, 4(4), 351–355.

- 484 McRae, B. H., & Beier, P. (2007). Circuit theory predicts gene flow in plant and animal  
485 populations. *Proceedings of the National Academy of Sciences*, 104(50), 19885–19890.
- 486 Naimi, B. (2015). R package: "usdm": <https://cran.r-project.org/package=usdm>
- 487 Oliver TH, MD Morecroft (2014) Interactions between climate change and land use change on  
488 biodiversity: attribution, problems, risks, and opportunities. *WIREs Climate Change*  
489 5:317-335.
- 490 Penuelas J, J Sardans, M Estiarte, R Aogaya, J Carnicer, M Coll, A Barbeta, A Rivas-Ubach, J  
491 Jlusia, M Garbulsky, J Filella, AS Jump (2013) Evidence of current impact of climate  
492 change on life: a walk from gene to the biosphere. *Global Change Biology* 19:2303-2338.
- 493 Phillips, S. J., Anderson, R. P., & Schapire, R. E. (2006). Maximum entropy modeling of species  
494 geographic distributions. *Ecological Modelling*, 190(3–4), 231–259.  
495 <https://doi.org/10.1016/j.ecolmodel.2005.03.026>
- 496 PRISM Climate Group. (2012). United States 30-yr Normals: precipitation, minimum  
497 temperature, maximum temperature 1981-2010. available online:  
498 <http://prism.oregonstate.edu>. Oregon State University, Corvallis, OR, USA.
- 499 Piou, C., Taylor, M. H., Papaix, J., & Prévost, E. (2015). Modelling the interactive effects of  
500 selective fishing and environmental change on Atlantic salmon demogenetics. *Journal of*  
501 *Applied Ecology*, 52(6), 1629–1637. <https://doi.org/10.1111/1365-2664.12512>
- 502 Rice, S., & Clark, R. W. (2017). Elucidating dispersal ecology of reclusive species through  
503 genetic analyses of parentage and relatedness: the island night lizard (*Xantusia*  
504 *riversiana*) as a case study. <https://doi.org/10.1101/125666>
- 505 Rice, S. E., & Clark, R. W. (2016). Factors affecting intra-island genetic connectivity and  
506 diversity of an abundant and widespread island endemic, the San Clemente Island night  
507 lizard. *bioRxiv*, 060038.
- 508 Rico, Y. (2017). Using computer simulations to assess sampling effects on spatial genetic  
509 structure in forest tree species. *New Forests*, 48(2), 225-243. [https://doi.org/10.1007/s11056-](https://doi.org/10.1007/s11056-017-9571-y)  
510 [017-9571-y](https://doi.org/10.1007/s11056-017-9571-y)
- 511 Row, J. R., Wilson, P. J., Gomez, C., Koen, E. L., Bowman, J., Thornton, D., & Murray, D. L.  
512 (2014). The subtle role of climate change on population genetic structure in Canada lynx.  
513 *Global Change Biology*, 20(7), 2076–2086. <https://doi.org/10.1111/gcb.12526>

- 514 Smith, H. M. (1946). A subspecies of the lizard *Xantusia riversiana*. *Journal of the Washington*  
515 *Academy of Sciences*, 36(11), 392–393.
- 516 Swab, R. M., Regan, H. M., Matthies, D., Becker, U., & Bruun, H. H. (2015). The role of  
517 demography, intra-species variation, and species distribution models in species'  
518 projections under climate change. *Ecography*, 38(3), 221–230.  
519 <https://doi.org/10.1111/ecog.00585>
- 520 United States Fish and Wildlife Service (2014). Island night lizard (*Xantusia riversiana*) final  
521 Post-Delisting Monitoring Plan. U.S. Fish and Wildlife Service, Carlsbad Fish and  
522 Wildlife Office, Carlsbad, California.
- 523 United States Geological Survey. (2017). 3D Elevation Program (3DEP). available online:  
524 <https://nationalmap.gov/3DEP/index.html>
- 525 Zweifel, R. G., & Lowe, C. H. (1966). The Ecology of a Population of *Xantusia vigilis*, the  
526 Desert Night Lizard. *American Museum Novitates*, 2247, 1–57.
- 527

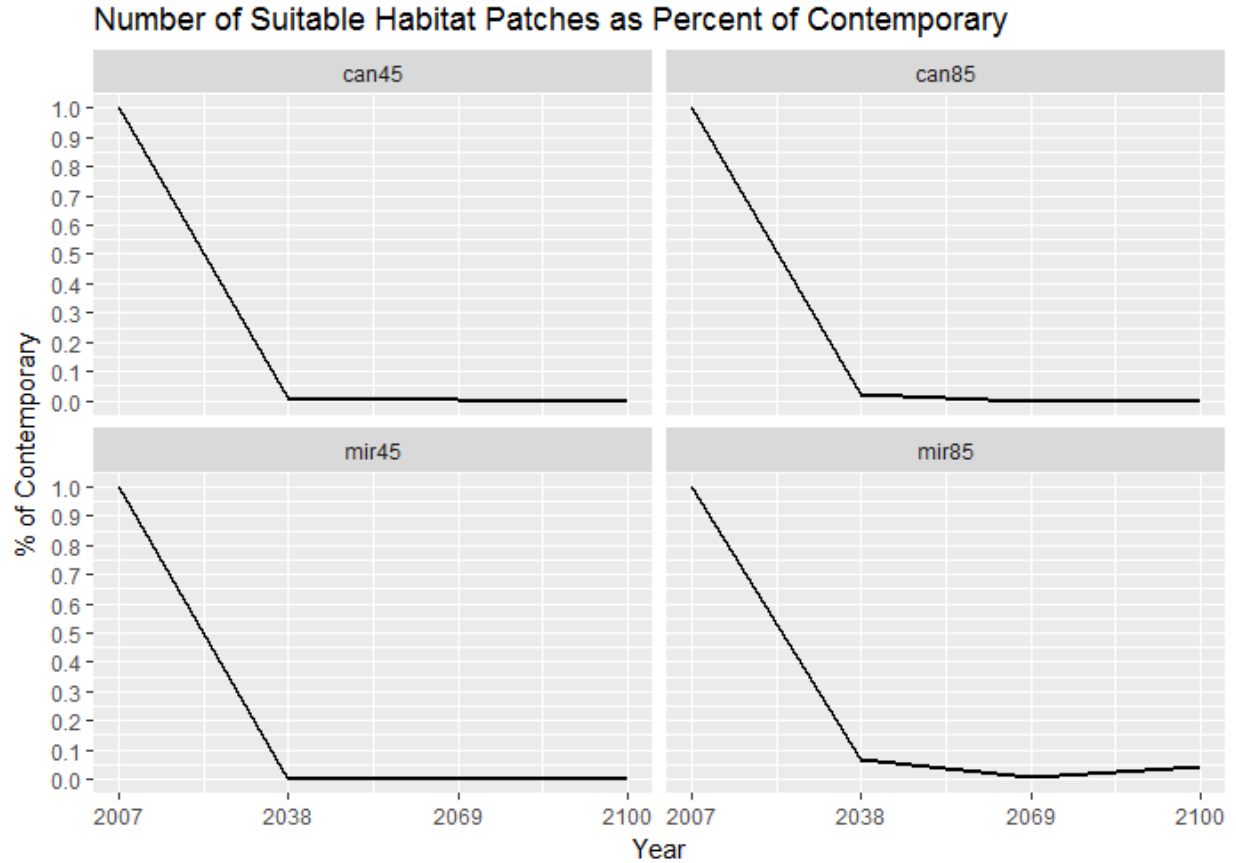
528 **Table 1:** Environmental and topographic predictors. Predictors were retained for models of SBI  
 529 and SCI based on stepwise VIF. MAXENT calculated percent contribution and permutation  
 530 importance for each variable.

Variable	Description	Percent Contribution	Permutation Importance
Bio9	Mean temperature of driest quarter	26.6	30.8
Bio15	Precipitation seasonality	12.6	4.7
Bio3	Isothermality	11.9	15.2
Bio6	Minimum temperature of coldest month	9.2	6.1
Bio5	Maximum temperature of warmest month	8	8.5
TPI	Topographic position	7.8	5
Aspect	Direction slope faces	7.2	7.4
Bio14	Precipitation of driest month	6.5	11.3
Slope	Elevational steepness	5.1	4.9
Bio18	Precipitation of warmest quarter	5	6.1

531  
 532 **Table 2:** Proportional EMA by year, climate change scenario, and model. Simulation averaged  
 533 proportional EMA between the observed minimum abundance between the contemporary model  
 534 (2007) and the endpoint, over 100 stochastic simulations. Climate models were CanESM and  
 535 Miroc with 2 RCPS, 4.5 and 8.5, and a null model of stable contemporary conditions. The  
 536 distance model refers to the stable geographic equivalent resistance model and connective model  
 537 refers to variable effective distances between patches.

Climate Model	Distance Model			Connectivity Model		
	2038	2069	2100	2038	2069	2100
CanESM 4.5	15.790	2.819	0.150	16.181	1.961	0.082
CanESM 8.5	23.403	0.379	0.000	24.175	0.299	0.000
Miroc 4.5	8.065	1.354	0.094	8.269	0.747	0.044
Miroc 8.5	57.000	8.828	1.760	57.139	8.696	0.924
No Change	92.920	90.688	89.840	94.056	92.747	91.547

538



539

540

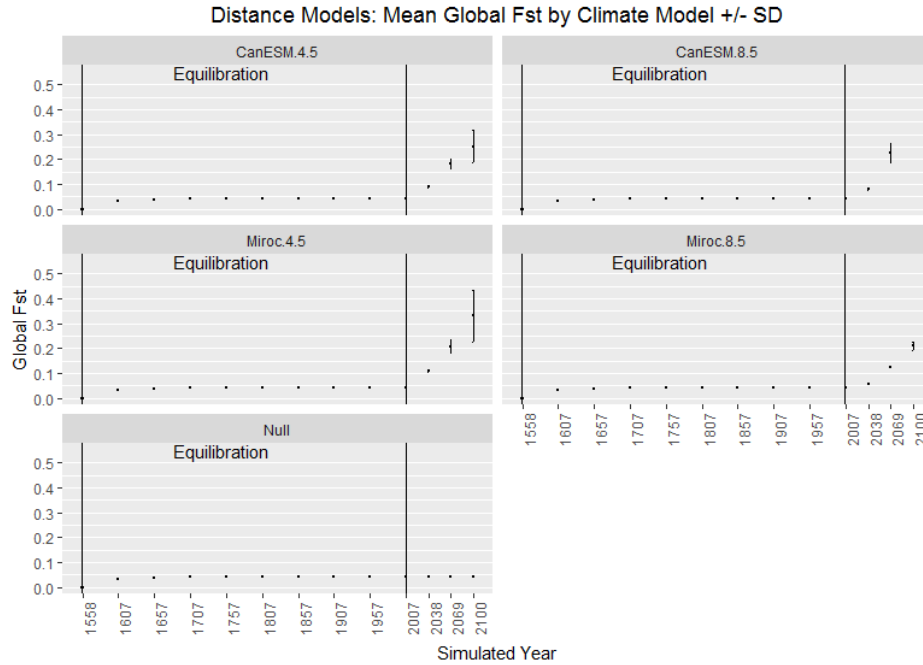
541 Figure 1: Percentage of Contemporary Suitable Habitat Patches Remaining on both SBI and SCI.

542 Habitat patches were defined based on an observed occupancy value of 0.1095 with the % of

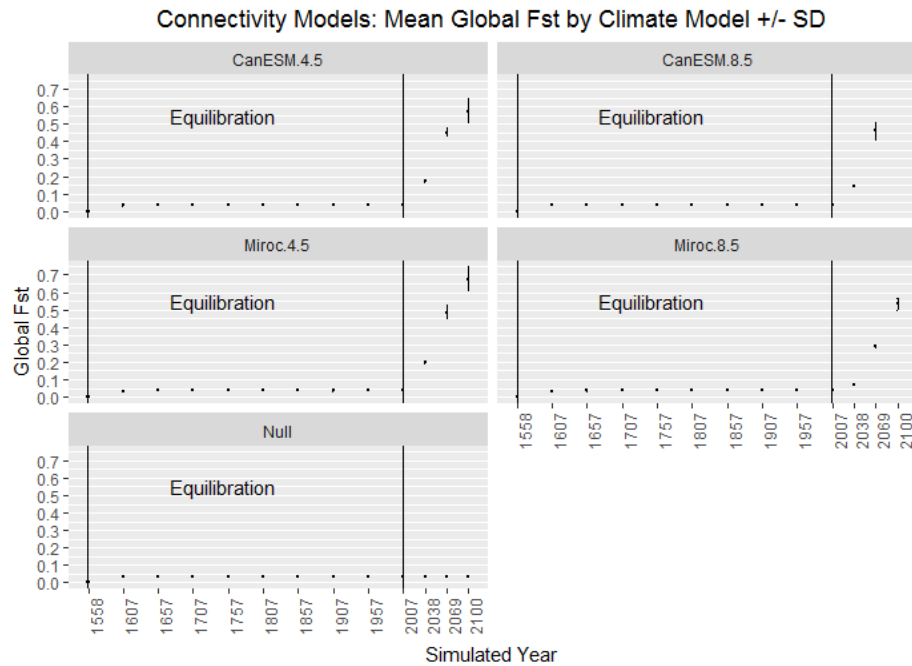
543 contemporary values representing percentages 0 to 1.

544



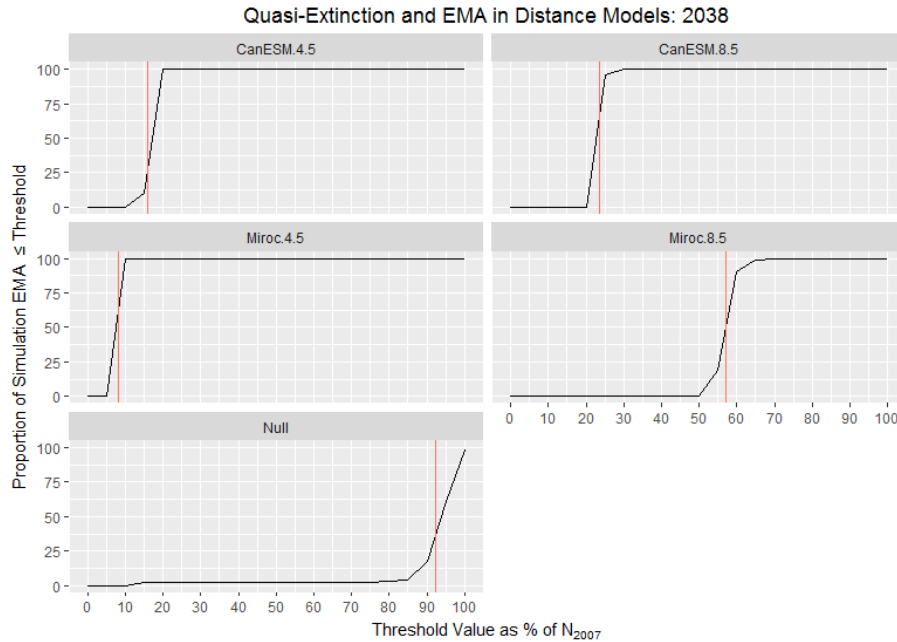


545

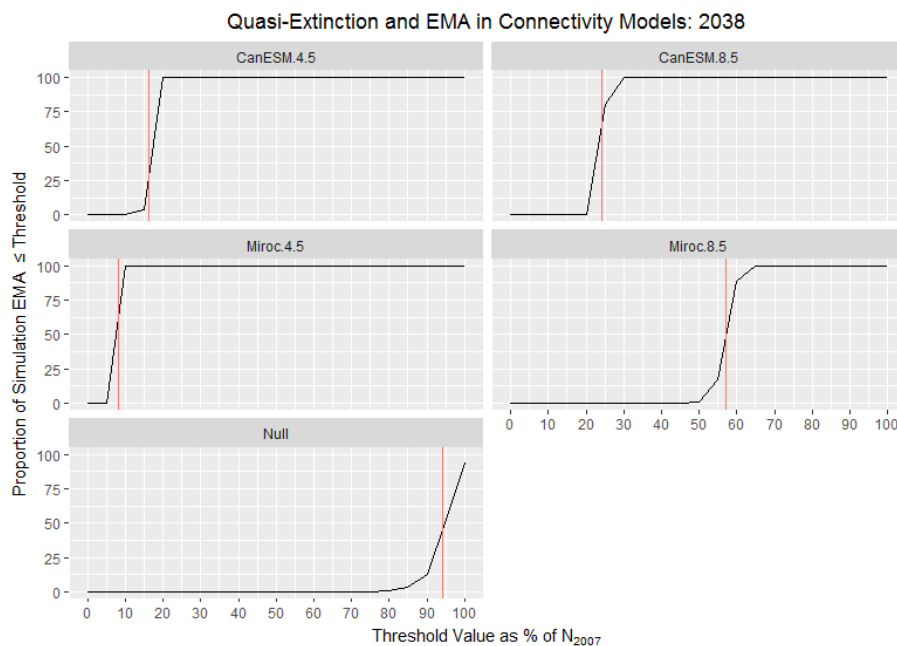


546

547 Figure 2: Mean global Fst with standard deviations. Distance-based models (top) and  
 548 connectivity models (bottom) listed with climate model identification with RCP is given in the  
 549 title. The Y-axis is global Fst averaged over all simulations for each model with error bars  
 550 indicating standard deviation of the mean. Vertical lines denote the range considered for model  
 551 equilibrium. Mean Fst is denoted with +/- standard deviations plotted from point data from  
 552 sampled time points (X-axis).



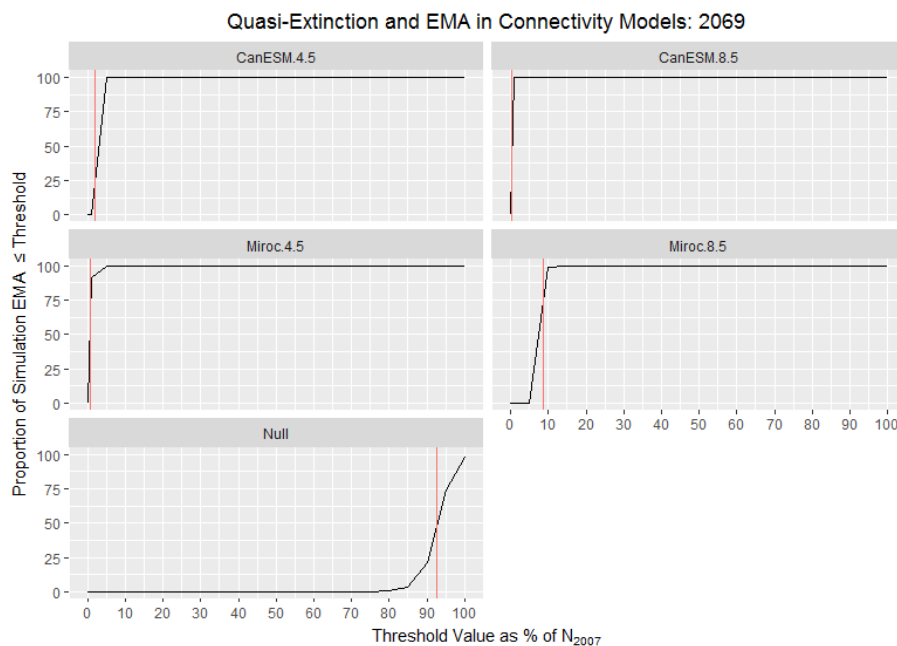
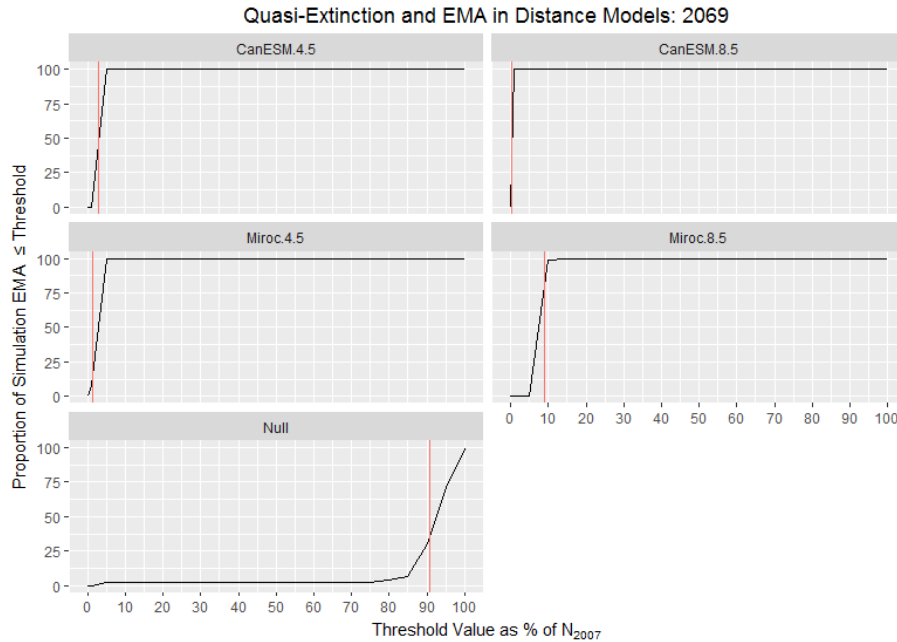
553



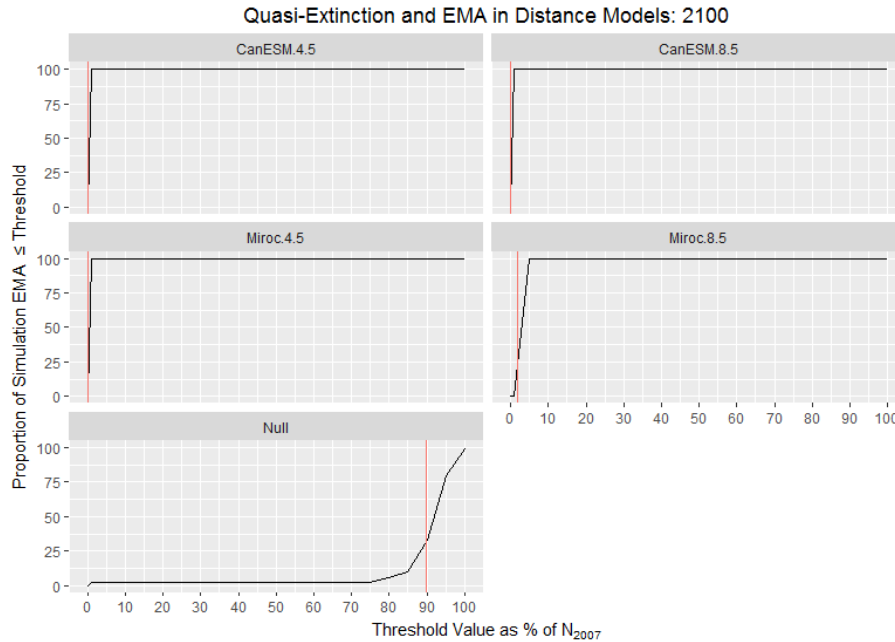
554

555

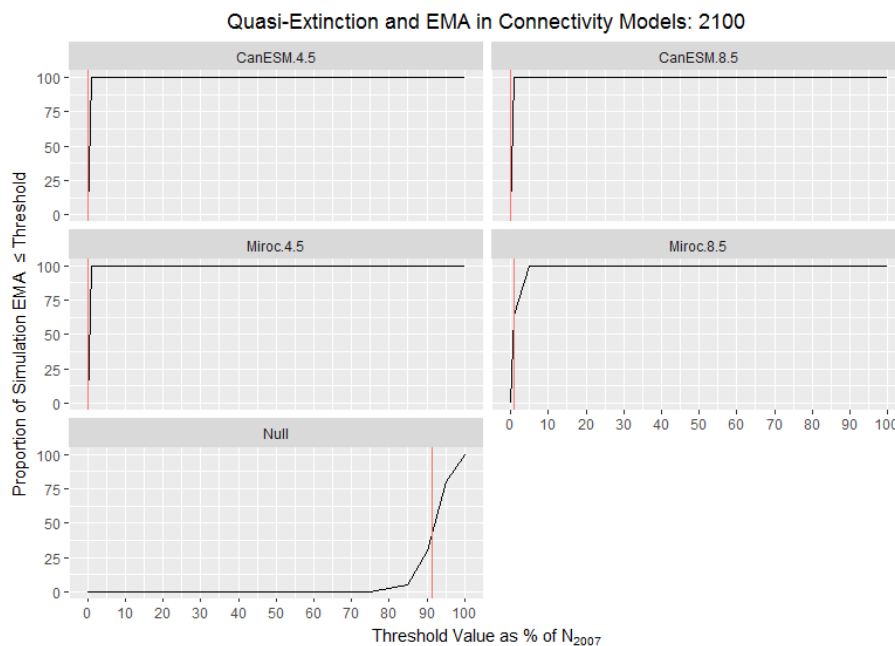
556 Figure 3: Quasi-extinction for distance and connectivity models 2007-2038. Distance-based  
557 models (top) and connectivity models (bottom) listed with climate model identification with RCP  
558 is given in the title. The Y-axis represents risk, defined as the proportion of models with a  
559 minimum size, represented as the proportion of the 2007 census population size remaining, less  
560 than or equal to the threshold value (X-axis). The red vertical line represents the proportional  
561 EMA averaged across all runs for a given model.



565 Figure 4: Quasi-extinction for connectivity models 2007-2069. Distance-based models (top) and  
566 connectivity models (bottom) listed with climate model identification with RCP is given in the  
567 title. The Y-axis represents risk, defined as the proportion of models with a minimum size,  
568 represented as the proportion of the 2007 census population size remaining, less than or equal to  
569 the threshold value (X-axis). The red vertical line represents the proportional EMA averaged  
570 across all runs for a given model.



571



572

573 Figure 5: Quasi-extinction for connectivity models 2007-2100. Distance-based models (top) and  
574 connectivity models (bottom) listed with climate model identification with RCP is given in the  
575 title. The Y-axis represents risk, defined as the proportion of models with a minimum size,  
576 represented as the proportion of the 2007 census population size remaining, less than or equal to  
577 the threshold value (X-axis). The red vertical line represents the proportional EMA averaged  
578 across all runs for a given model.

579

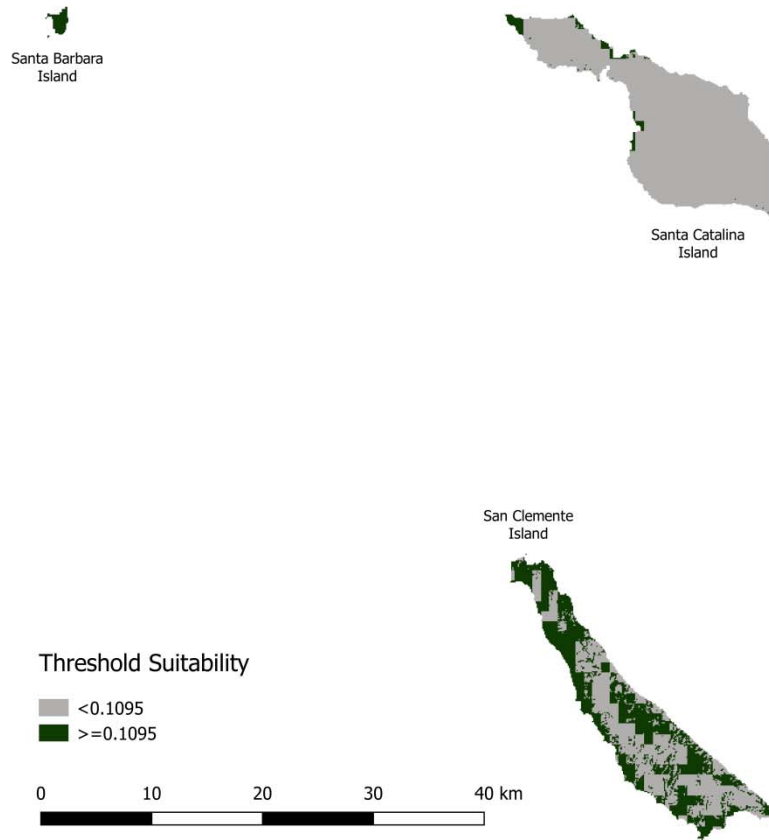
580 Supplemental Tables and Figures:

581

582 Table S1: Demographic model

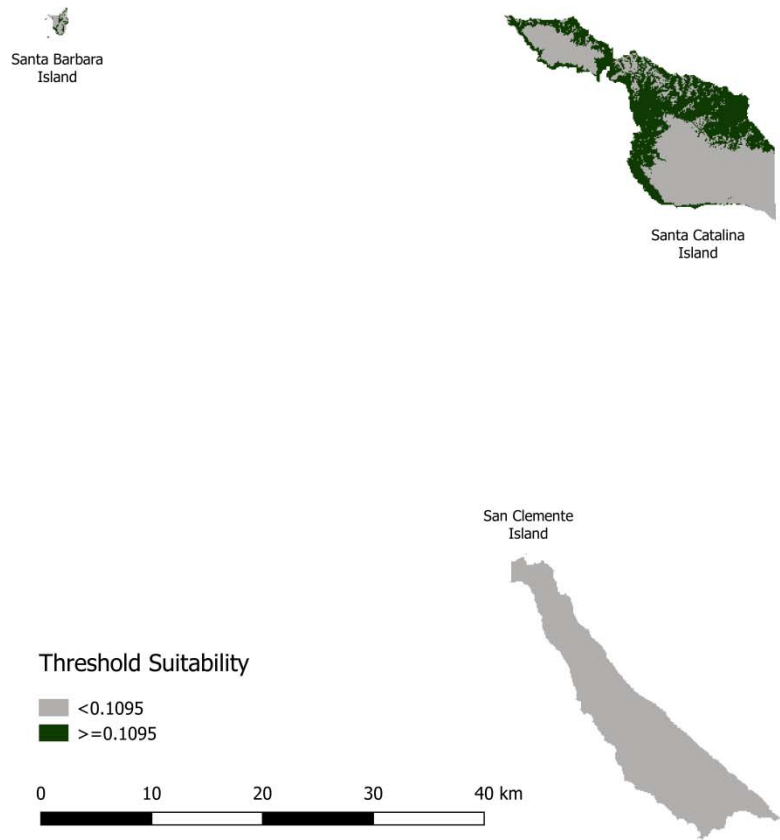
<b>Age Class</b>	<b>Mortality (SD)</b>	<b>Male Maturity</b>	<b>Female Maturity</b>	<b>Fecundity (SD)</b>
0	11.7 (13.45)	0	0	0
1	16.3 (16.05)	0	0	0
2	19.5 (21.15)	0.5	0	0
3	15.6 (18.63)	1.0	1.0	3.9 (1.15)

Figures: S1-S13 Habitat suitability models based on Threshold for all models in range. Models are identified by the endpoint, followed by the model name and RCP. Dark patches indicate suitable habitat based on the 0.1095 threshold value. Gray indicates unsuitably habitat below the threshold.

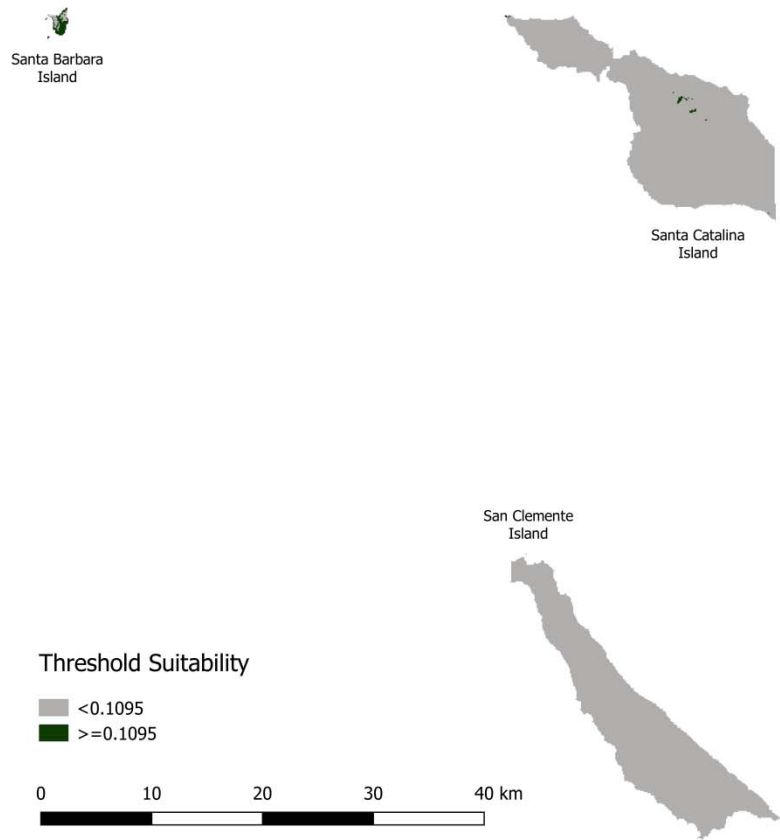


S1: Contemporary

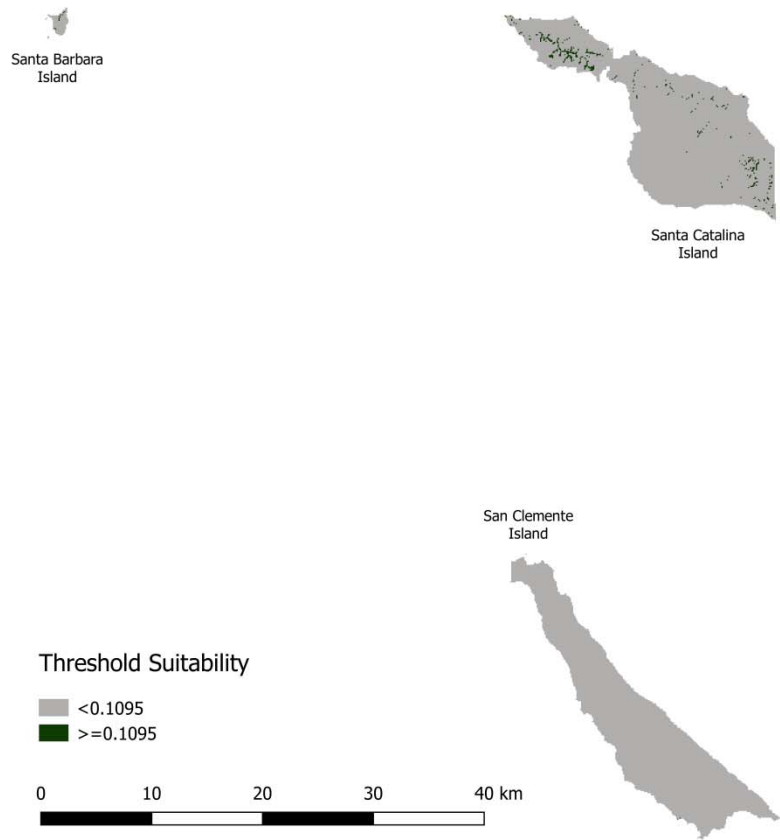




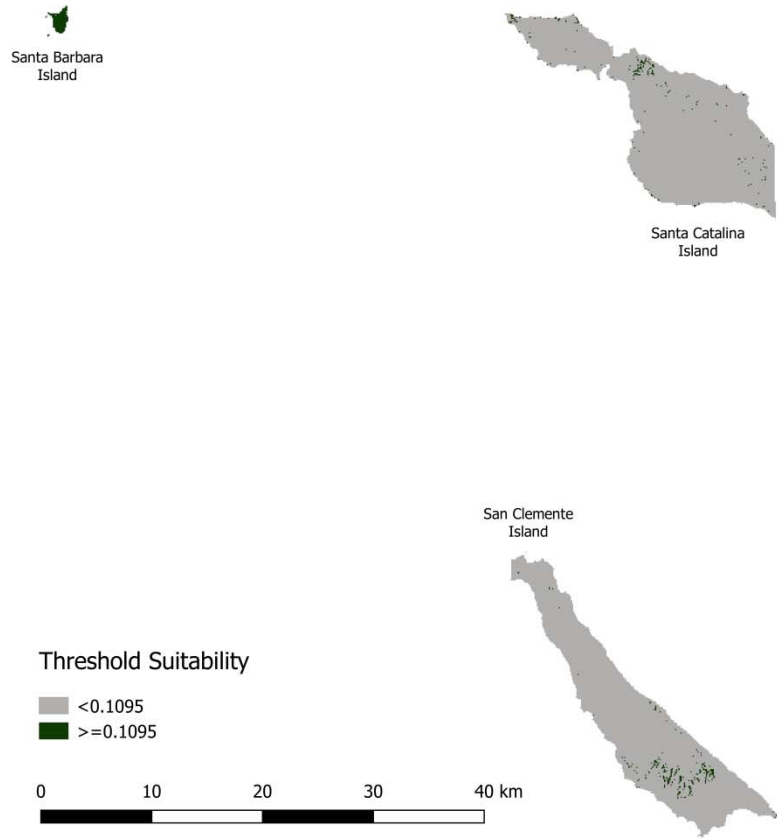
S2: 2038, CanESM 4.5



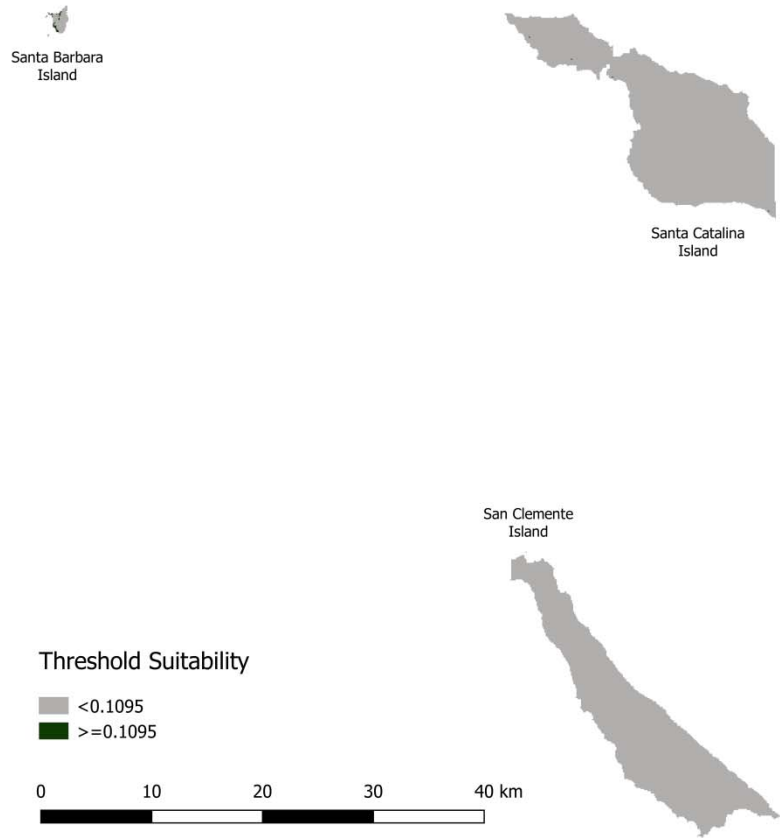
S3: 2038, CanESM 8.5



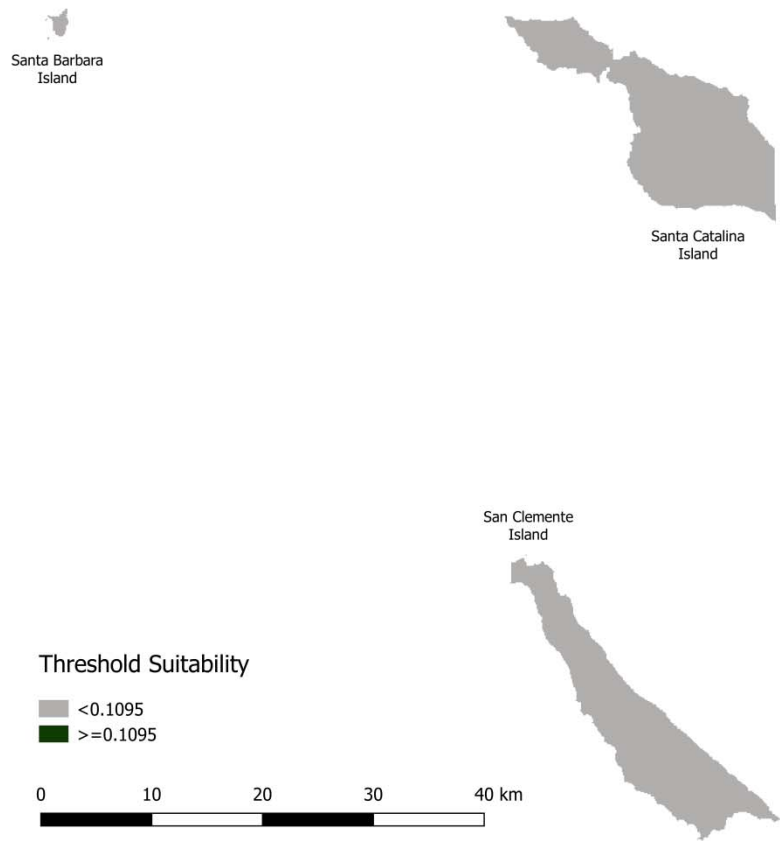
S4: 2038, Miroc 4.5



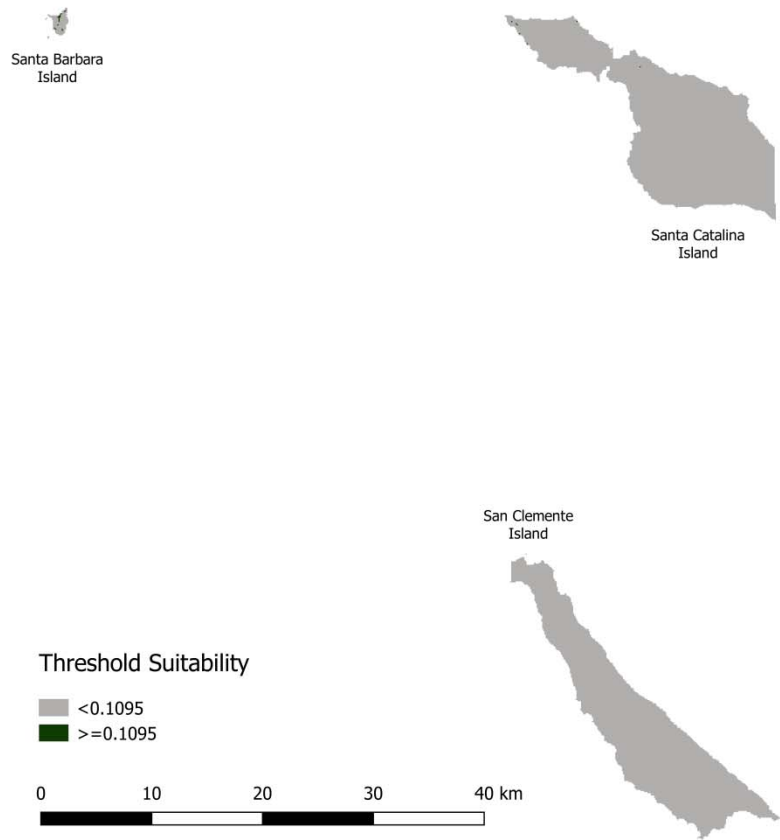
S5: 2038, Miroc 8.5



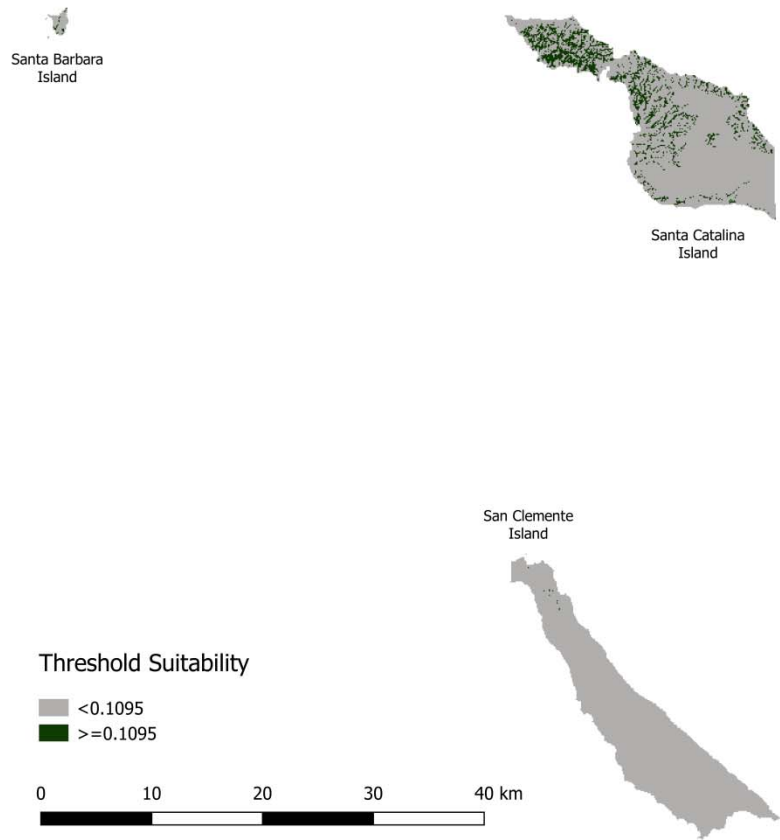
S6: 2069, CanESM 4.5



S7: 2069, CanESM 8.5

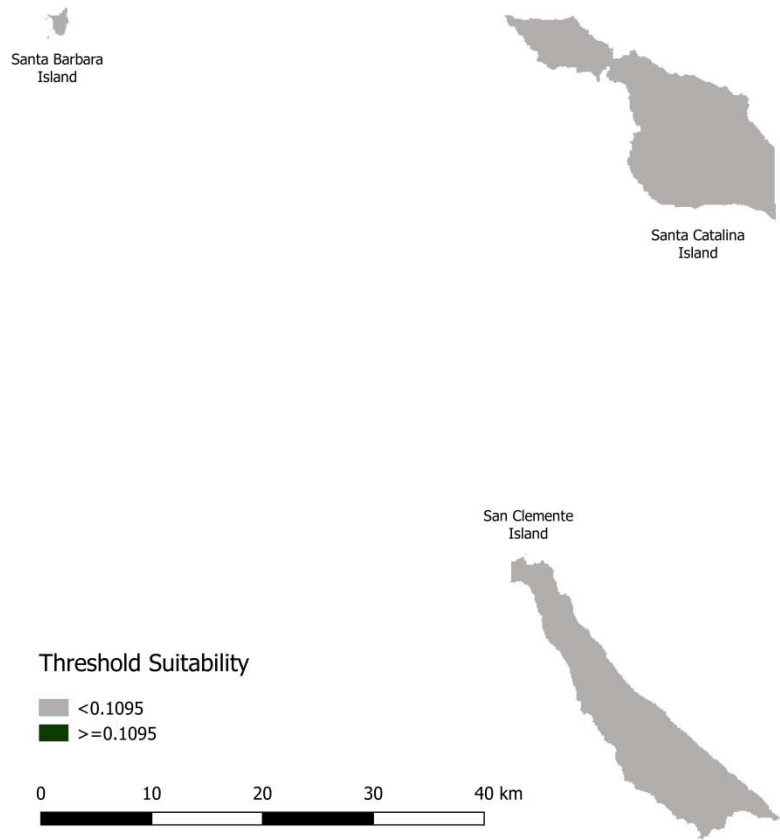


S8: 2069, Miroc 4.5

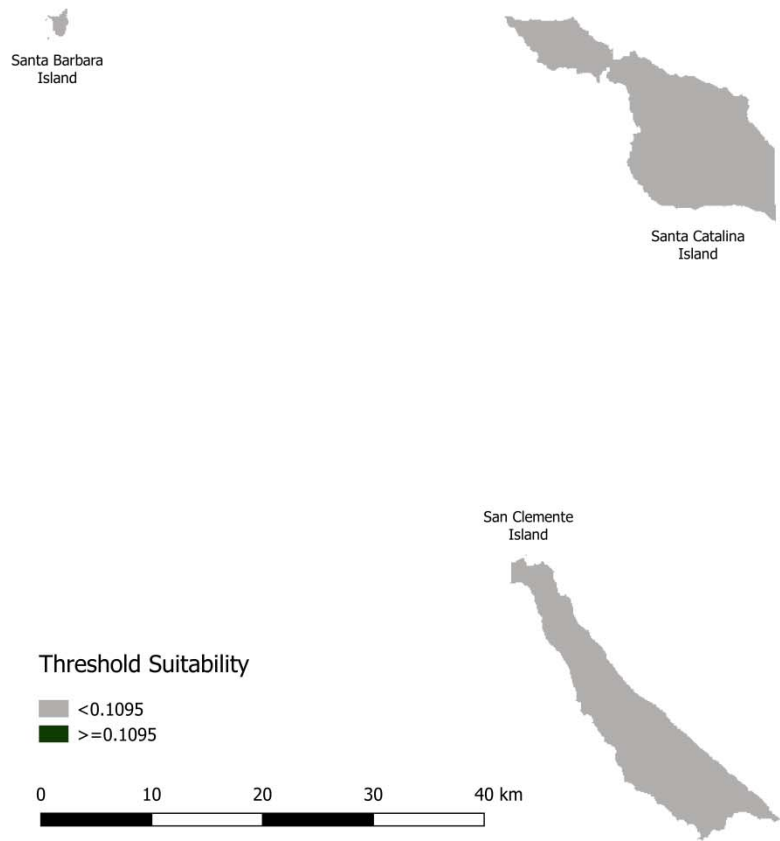


S9: 2069, Miroc 8.5

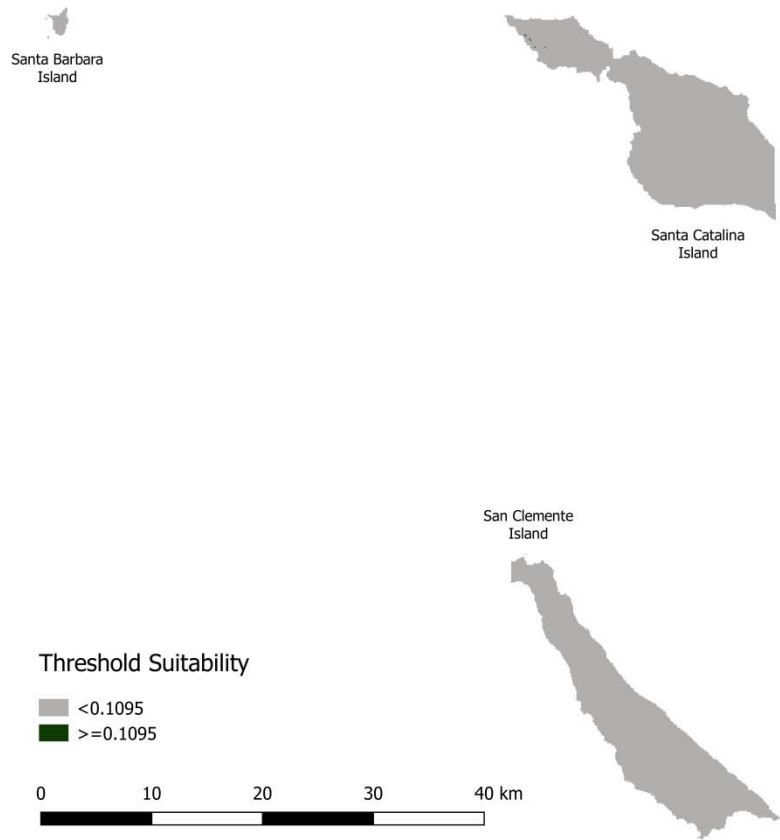




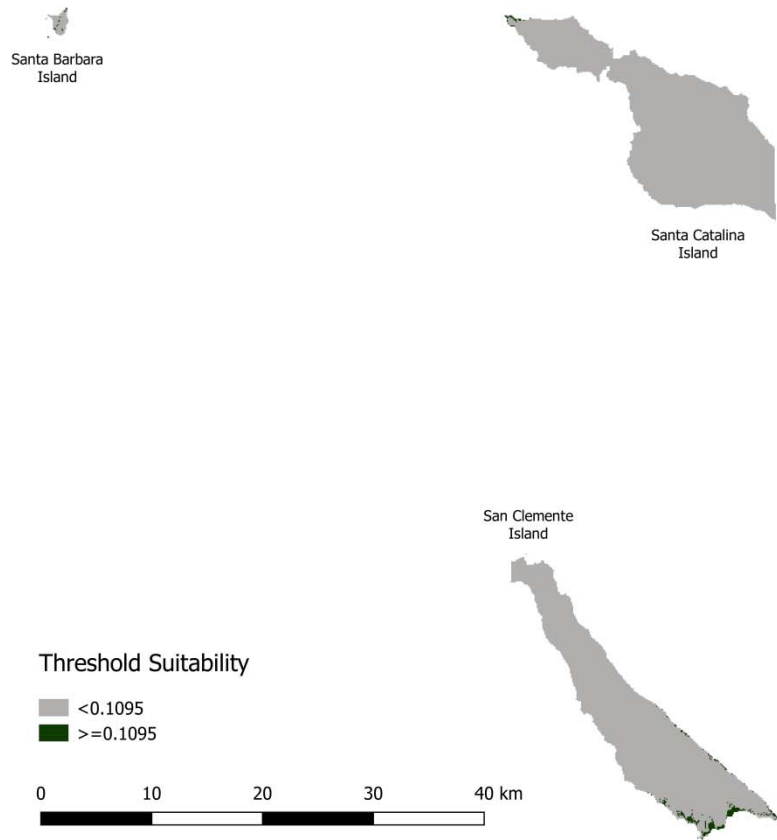
S10: 2100, CanESM 4.5



S11: 2100, CanESM 8.5



S12: 2100, Miroc 4.5



S13: 2100, Miroc 8.5